ARTICLE

Real-time and dynamic estimation of CO_2 emissions from China's lakes and reservoirs

Kun Sun,[1] Junjie Jia,[1,2] Shuoyue Wang,[1,2] and Yang Gao[1,2,*]
*Correspondence: gaoyang@igsnrr.ac.cn (Y.G.)
Received: April 15, 2023; Accepted: November 8, 2023; Published Online: November 10, 2023; https://doi.org/10.59717/j.xinn-geo.2023.100031

GRAPHICAL ABSTRACT

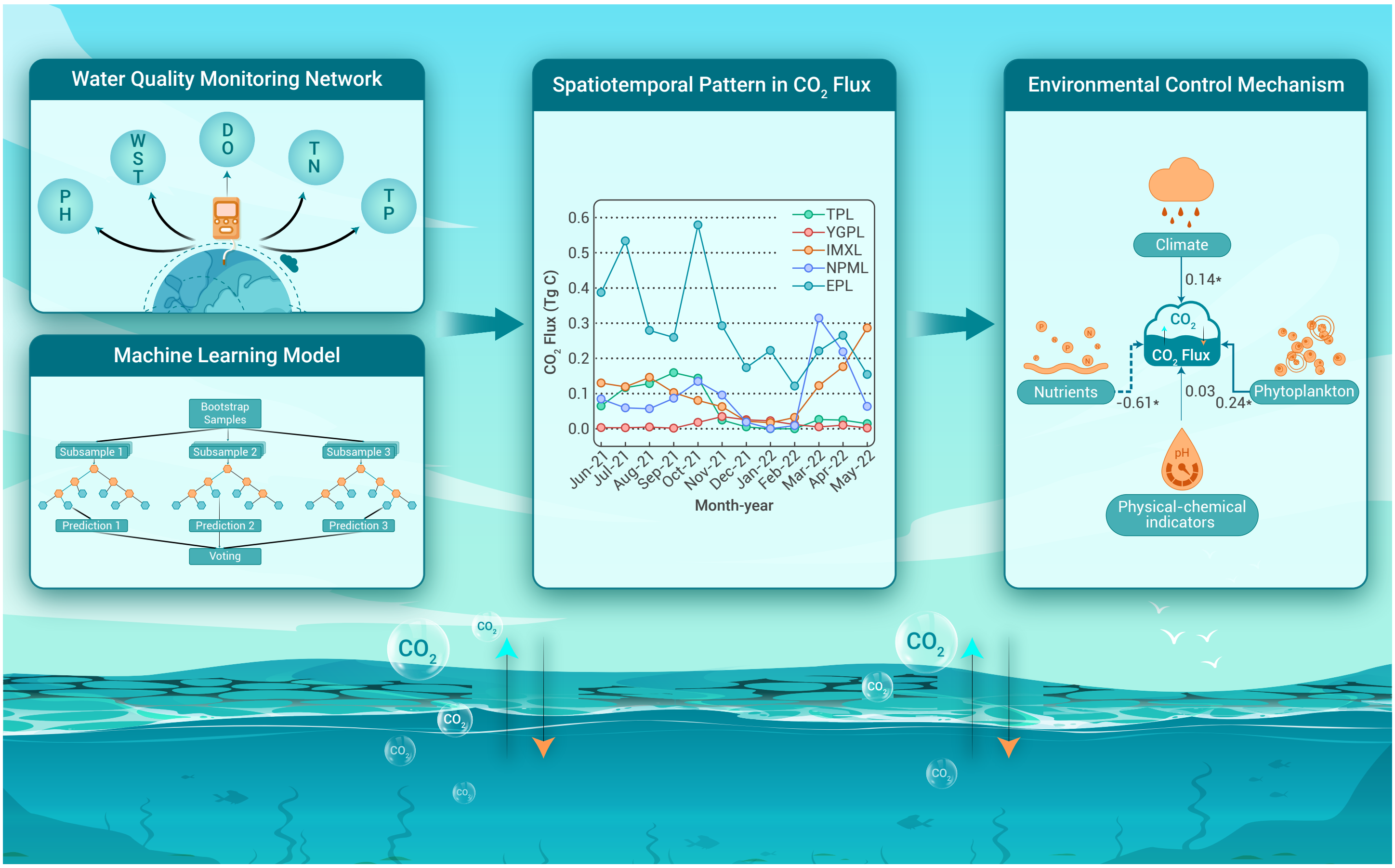

PUBLIC SUMMARY

- Lake CO_2 emissions were estimated using real-time water quality monitoring data.
- China's total lake and reservoir CO_2 emission between 2021-2022 was 6.78 Tg C yr^{-1}.
- General environmental controls were pH, dissolved oxygen, and air temperature.

Real-time and dynamic estimation of CO_2 emissions from China's lakes and reservoirs

Kun Sun,[1] Junjie Jia,[1,2] Shuoyue Wang,[1,2] and Yang Gao[1,2,*]

[1]Institute of Geographic Sciences and Natural Resources Research, Chinese Academy of Sciences, Beijing 100101, China

[2]University of Chinese Academy of Sciences, Beijing 100049, China

*Correspondence: gaoyang@igsnrr.ac.cn (Y.G.)

Received: April 15, 2023; Accepted: November 8, 2023; Published Online: November 10, 2023; https://doi.org/10.59717/j.xinn-geo.2023.100031

Citation: Sun K., Jia J., Wang S., et al., (2023). Real-time and dynamic estimation of CO_2 emissions from China's lakes and reservoirs. The Innovation Geoscience 1(3), 100031.

Lakes and reservoirs act as active carbon (C) reactors and regulators. Both play a crucial terrestrial ecosystem C balance role via carbon dioxide (CO_2) exchange processes across the water-air interface. It has previously been confirmed that CO_2 flux from lakes and reservoirs generally exhibits significant spatiotemporal heterogeneity. Nevertheless, spatiotemporal CO_2 flux variation has seldom been considered in global and regional CO_2 emission estimates from lakes and reservoirs. By accounting for spatiotemporal CO_2 flux and water surface area variability, we evaluated spatial and temporal CO_2 emission dynamics from China's inland lakes and reservoirs using national real-time water quality monitoring data and machine learning (ML) models. Between 2021–2022, we estimated total C emission flux at 6.78 (±2.5) Tg C yr^{-1}, where seasonal and regional distribution both exhibited significant heterogeneity. Our state-of-the-art estimate is significantly lower than previous estimates of 7.9~25 Tg C yr^{-1} from the 1980s to the 2010s. Water quality parameters (pH and dissolved oxygen [DO]) and climate factors (air temperature) were identified as the general environmental CO_2 flux controls. For the first time, this study clarifies the spatiotemporal patterns and drivers of CO_2 flux from China's inland lakes and reservoirs, providing a more complete C budget picture of China's aquatic ecosystems.

INTRODUCTION

Carbon dioxide (CO_2) exchange across the water-air interface, quantified using CO_2 flux, plays an important role in aquatic carbon (C) cycling processes.[1-3] In inland water, the absorption and release of CO_2 are determined by primary biogeochemical cycling processes, including phytoplankton photosynthesis, photochemical mineralization of dissolved organic carbon (DOC), and microbial respiration during DOC decomposition, all of which are extremely sensitive to multiple environmental stressors (i.e., wind, sunlight, temperature, and nutrients).[4,5] Moreover, CO_2 exchange from lakes and rivers is also significantly influenced by surrounding landscape patterns.[6-8] Complex environmental control mechanisms lead to significant spatiotemporal CO_2 exchange variability. Both long-term and direct observations taken from individual lakes and reservoirs have shown that CO_2 flux exhibits dramatic fluctuations at diel, seasonal, and annual scales as well as significant spatial disparity.[9-13] However, under observational restrictions, our understanding of spatiotemporal lake and river CO_2 flux patterns is fragmented.[14] Hence, capturing spatiotemporal CO_2 flux dynamics at the water-air interface is of great importance to inland water C budget assessments.[15]

Global and regional CO_2 emission estimates from lakes and reservoirs have generally been scaled from collected site-level measurements, most of which had a sparse and heterogeneous spatial distribution, a prolonged timespan, and a dominance of diurnal observations.[13,16] Moreover, upscaling spatiotemporally discrete CO_2 flux measurements to regional and global scales may cause widespread uncertainty in evaluating total CO_2 emissions from inland waterbodies.[13,17,18] A recent global compilation of high-frequency CO_2 measurements from rivers indicated that nocturnal CO_2 emissions were significantly higher than diurnal emissions in temperate regions, while diel changes were much lower in boreal and tropical regions.[7,19] Global CO_2 emissions from rivers (0.65–1.8 Pg C yr^{-1}) would increase by 0.2–0.55 Pg C yr^{-1} when accounting for such high nocturnal emissions.[19] Monthly CO_2 emissions from global rivers have also exhibited considerable fluctuation, ranging from 112 to 209 Tg C.[20] To date, spatiotemporal CO_2 flux variation has rarely been accounted for in total CO_2 emission estimates from inland lakes and reservoirs at regional or global scales.[16-18,21] Furthermore, satellite observations have demonstrated that variation in the surface extent of seasonal lakes and reservoirs is of particular interest, whose influence on upscaling CO_2 flux may be consequential.[22,23] Reservoirs and ponds that seasonally dry up (i.e., non-running inland water) have been recognized as CO_2 emission hotspots. Moreover, global CO_2 emissions from reservoir drawdown areas have reached 26.2 Tg C yr^{-1}, increasing reservoir CO_2 emissions by 53%.[24] Although small ponds only account for 8.6% of all lakes and ponds globally, they contribute 15.1% of the total CO_2 emissions.[25] Overall, global CO_2 emissions from inland lakes and reservoirs have been estimated to be between 0.32 and 0.64 Pg C yr^{-1}.[13,26] However, there remains a large degree of uncertainty in CO_2 emission estimates from non-running inland water globally. This uncertainty is largely due to the absence of spatiotemporally dynamic CO_2 flux and water surface area data during the upscaling process as well as CO_2 emission overestimations from small lakes and lakes in tropical regions.[16,23]

China is home to thousands of lakes and reservoirs (Figure S1), only accounting for ~1% of its total land area. However, these lakes and reservoirs could offset the C sink capacity of China's terrestrial ecosystems by 4–6%.[14,17] Nationally, total CO_2 emissions from lakes and reservoirs were estimated between 7.9 and 25 Tg C yr^{-1}.[17,18,21] These estimates were mostly based on field observations during specific time periods and whose CO_2 flux estimation precision has generally been considered acceptable, largely based on their direct measurements. However, they do not reflect temporal CO_2 flux dynamics due to their lack of continuous observations. Total CO_2 emissions from China's lakes and reservoirs have increased from 9.4 Tg C yr^{-1} in the 1980s to 12.1 Tg C yr^{-1} in the 2010s, while drivers that control spatiotemporal CO_2 emission transformation processes remain unclear.[18] The diversity of geographical and climatologic factors in China's inland lakes and reservoirs leads to different controlling mechanisms in the CO_2 exchange. Many environmental factors (e.g., nutrient loading, thermal structure, and inorganic and hydrological processes) have been recognized as being major controlling CO_2 emission factors within individual lakes and reservoirs in China.[27-30] However, there remains a considerable knowledge gap concerning the general drivers that are used to explain CO_2 emission dynamics from China's inland lakes and reservoirs.

To address the spatial and temporal constraints of large-scale CO_2 emission estimations while offering a more complete understanding of how CO_2 emissions from lakes and reservoirs respond to global climate change, this study used national high-frequency water quality monitoring data with the support of satellite remote sensing imagery and machine learning (ML) models to provide the first real-time and dynamic estimates of CO_2 emissions from China's inland lakes and reservoirs. Based on these new estimates, this study aimed to (1) ascertain spatiotemporal CO_2 emission patterns from China's inland lakes and reservoirs and (2) determine the environmental controls on CO_2 exchange processes in non-running inland water.

RESULTS

Spatial and temporal F_c distribution

To better clarify diurnal differences in CO_2 exchange rates from China's inland lakes and reservoirs, diurnal and nocturnal site level CO_2 flux (represented by F_c) was compared among all 205 sampled sites (Figure 1). Mean diurnal F_c and mean nocturnal F_c values were mostly positive, indicating that most lakes and reservoirs acted as C sources (Figure 1A). Diurnal F_c values tended to be slightly higher than nocturnal F_c values in cases where the former was positive (Figure 1A and 1B), where maximum F_c values occurred most frequently at 12 and 8 a.m. (Figure 1C); diurnal F_c values tended to be

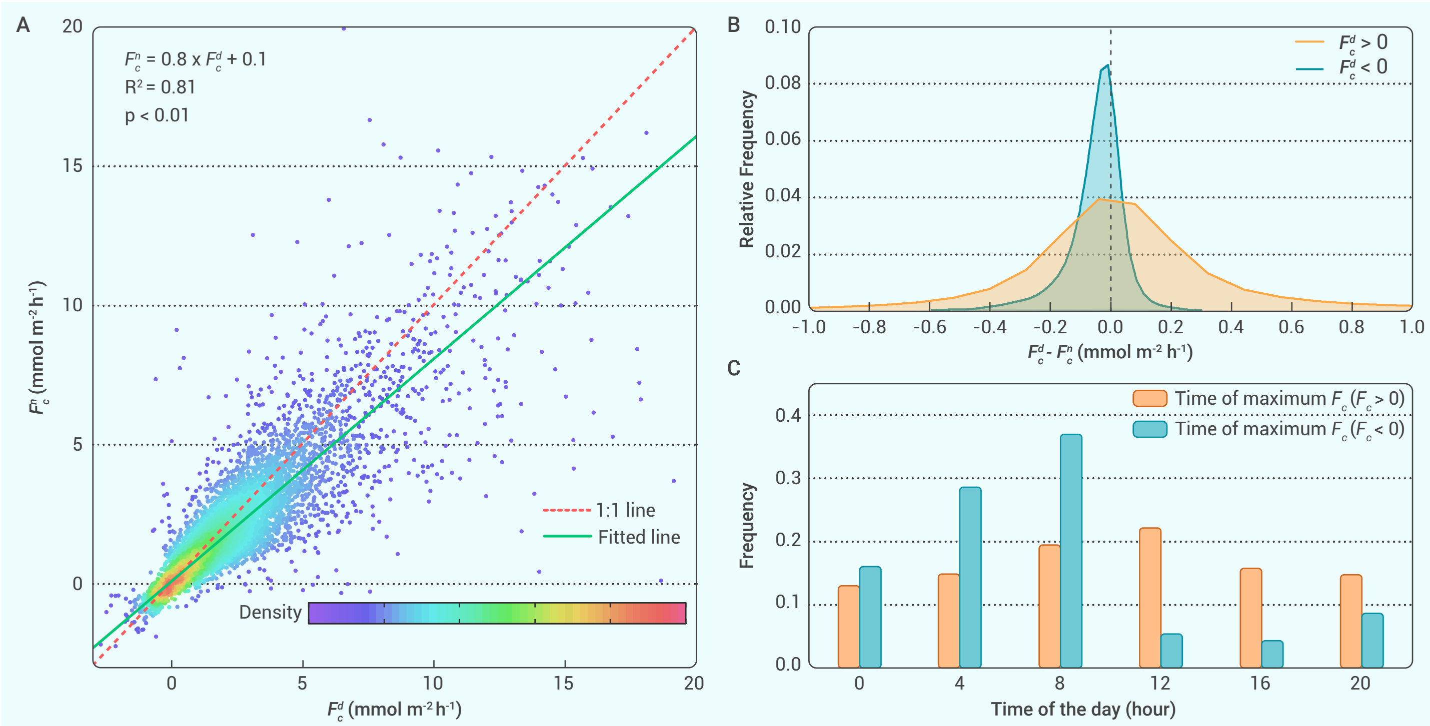

Figure 1. Diurnal F_c variation in sampled lakes and reservoirs (A) Relationship between mean diurnal F_c (*Fd c*) and mean nocturnal F_c (*Fn c*). (B) Distribution of differences between *Fd c* and *Fn c* (*Fd c-Fn c*) in cases where *Fd c*>0 and *Fd c*<0. (C) Distribution of time with maximum F_c in cases where F_c >0 and F_c <0.

lower than nocturnal F_c values in cases where the former was negative (Figure 1A and 1B), where maximum F_c values occurred most frequently at 8 and 4 a.m. (Figure 1C).

Seasonally, the partial pressure of CO_2 (pCO_2) in lakes and reservoirs varied from 4 to 10544 µatm, while mean pCO_2 values ranged between 827 and 1113 µatm. Moreover, 16.6~33.5% of all sampled lakes and reservoirs yielded pCO_2 values less than 400 µatm, indicating a state of CO_2 undersaturation (Figure S7). Moreover, F_c exhibited a lognormal distribution, and most F_c values were distributed in the range between 10 and 50 mmol m^{-2} d^{-1}, 16~34% of sampled lakes and reservoirs exhibited a negative seasonal mean F_c (Figure 2). Seasonal mean F_c fell in the range between 15 and 23.8 mmol m^{-2} d^{-1}, with a pattern of higher in summer and autumn, and lower in winter and spring. Our F_c estimates were comparable to those from previous observations (23~27 mmol m^{-2} d^{-1}).[18]

Regionally, stronger CO_2 emissions (>16 mmol m^{-2} d^{-1}) mainly occurred in eastern and northern China, including the Northeast Plain and Mountain Lake (NPML) zone, the Eastern Plain Lake (EPL) zone, and the Inner Mongolia-Xinjiang Lake (IMXL) zone. Conversely, CO_2 emissions from lakes and reservoirs in China's southwestern region, including the Yunnan-Guizhou Plateau Lake (YGPL) zone and the Tibetan Plateau Lake (TPL) zone, were generally weaker (<10 mmol m^{-2} d^{-1}) (Figure 3). This is consistent with regional pCO_2 distribution (Figure S8). Given that a large proportion of the population and industry activity is distributed in eastern China, lakes and reservoirs in eastern regions generally suffer from higher C and nutrient input intensity, which largely explains the significant regional difference in the CO_2 emission.[31,32]

CO_2 emissions from China's lakes and reservoirs

This study estimated total monthly CO_2 flux from lakes and reservoirs across five lake zones of China from June 2021 to May 2022 (Figure 4). Overall, the total CO_2 emission from these lakes and reservoirs was 6.78 (±2.5) Tg C yr^{-1} (Table 1). Regionally, more than half of all relevant CO_2 emissions originated from the EPL zone, where both F_c and water surface area ranked second among all five lake zones. The NPML and TPL zones yielded the highest F_c value (26.3 mmol m^{-2} d^{-1}) and water surface area (~4×10^4 km^2), respectively (Figure 3 and S1); however, NPML zone surface area and TPL zone F_c were both comparatively low, which resulted in their low total CO_2 emissions (i.e., 16.8% in the NPML zone and 10.4% in the TPL zone) (Figure 4B). Seasonally, only negligible differences in total CO_2 flux values were observed among spring, summer, and autumn (28~31%), while winter CO_2 emissions (10%) were clearly lower than that estimated from the other three seasons (Figure 4C). This decrease in winter CO_2 emission flux can largely be attributed to extensive lake and reservoir ice cover in northern China under frigid weather conditions, which could decrease winter CO_2 evasion by 1.32 Tg C yr^{-1} (Table S4, Supplemental Information S6). However, we also found that differences in seasonal CO_2 emission patterns were significant among all five lake zones (Figure 4A). In the EPL and TPL zones, CO_2 emission areal flux peaked in summer and autumn; in the NPML and IMXL zones, CO_2 emission areal flux peaked in spring.

Major environmental CO_2 emission controls

The geographical, hydrological, and climatological diversity of China's lakes and reservoirs is the reason behind the dramatic regional and climatic variation in their C cycling processes. For example, the associated thermal stratification structure of reservoirs has been reported to dominate CO_2 exchange processes in southwestern and southeastern China.[26,33] On the other hand, inorganic processes associated with pH have been shown as being the main controlling CO_2 absorption and emission factors in saltwater lakes within China's northern desert regions and the Tibetan Plateau.[29,34] For eutrophic lakes within the Yangtze River basin (e.g., Taihu Lake), CO_2 emissions are driven by eutrophication and temperature.[28,35] For floodplain lakes (e.g., Poyang Lake), CO_2 exchange has been shown to be driven by hydrological processes associated with water level fluctuation.[30,36]

Driving mechanisms associated with CO_2 exchange in China's inland lakes and reservoirs are known to be both complex and variable. Accordingly, this study explored the environmental controls on the pCO_2/F_c using structural equation modeling (SEM), and intended to reveal the general environmental and climatologic drivers of CO_2 exchange from inland lakes and reservoirs across China (Figure 5, Supplemental Information S7). The SEM was established on two dependent levels, allowing for different factor interactions on water pCO_2 and F_c. Among the nine significantly correlated environmental factors, water physicochemical indicators of pH and dissolved oxygen (DO) exhibited a strong negative effect on pCO_2. physio-chemistry indicators of water surface temperature (WST), electrical conductivity (EC) and turbidity (Turb), as well as nutrients of ammonia nitrogen (NH_3-N), total nitrogen (TN)

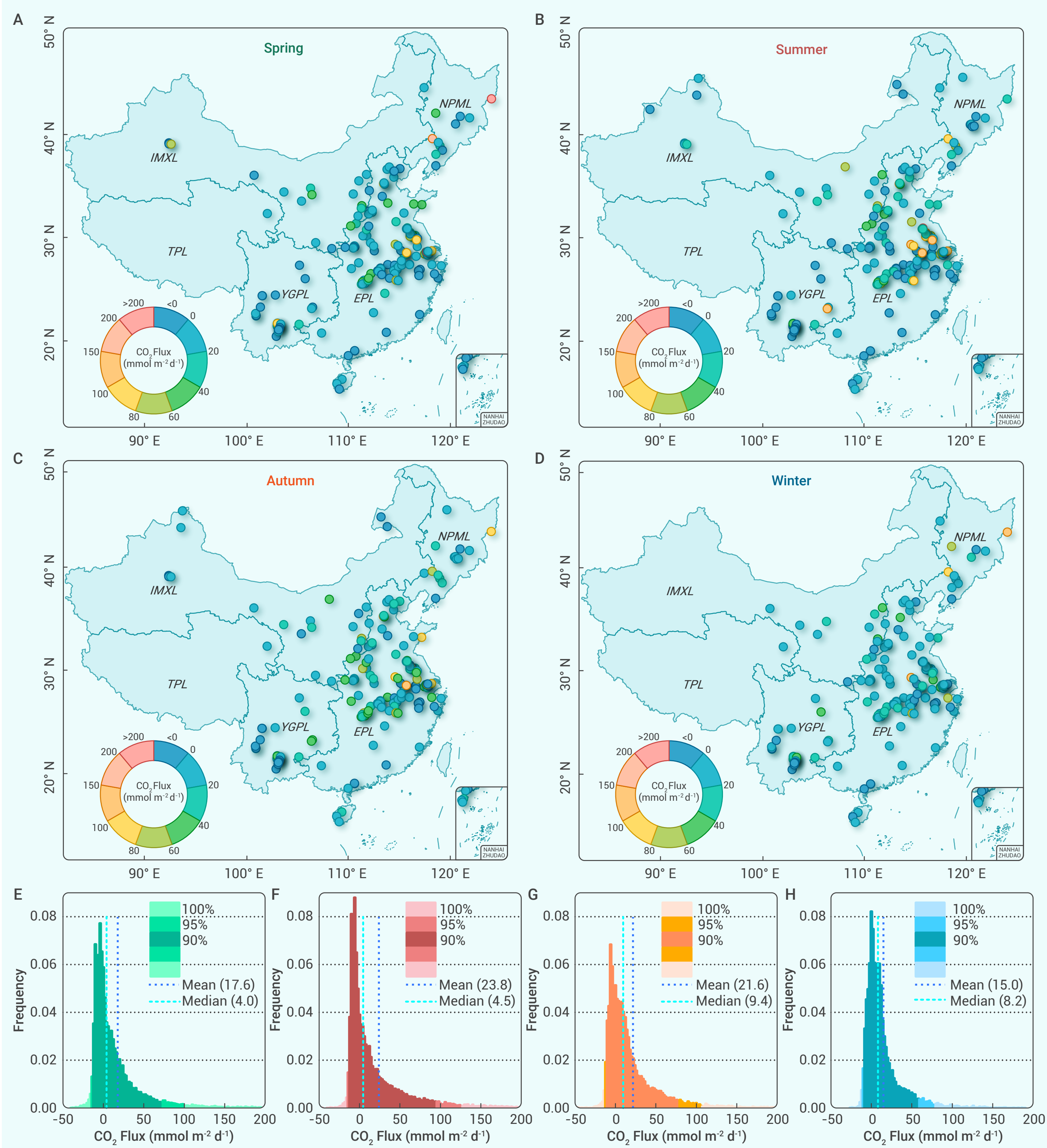

Figure 2. Seasonal distribution of F_c in China's inland lakes/reservoirs Subplots (A)–(D) and (E)–(H) denote spatial distributions and histograms of F_c during spring, summer, autumn, and winter, respectively. The dashed black and cyan lines denote means and medians of F_c, respectively, while shaded areas indicate 90% and 95% confidence intervals. The five lake zones labeled in the map represent the Tibetan Plateau Lake (TPL), the Yunnan-Guizhou Plateau Lake (YGPL), the Inner Mongolia-Xinjiang Lake (IMXL), the Northeast Plain and Mountain Lake (NPML), and the Eastern Plain Lake (EPL) zones, respectively. The four seasons were defined based on the standard meteorological season of the Northern Hemisphere (i.e., March, April, and May for spring; June, July, and August for summer; September, October, and November for autumn; December, January, and February for winter).

and total phosphorus (TP), showed a moderate positive effect on pCO_2. Phytoplankton (indicated by chlorophyll concentration, Chl-*a*) showed a weak effect on pCO_2. SEM results further suggested that F_c was primarily driven by pCO_2 in water, which explained 62% (square of the path coefficient) of F_c variance. Meteorological factors, especially wind speed (WS) at a 10 m height, had a relatively weaker positive effect on F_c. Although the negative correlation between pCO_2/F_c and water quality pH and DO parameters had previously been reported in specific lakes within the EPL and TPL zones,[29,34,36-38] our analysis suggested that the influence of this relationship may be more extensive. We also investigated environmental controls on pCO_2/F_c over different lake zones (Figure S11). pCO_2 showed stronger positive responses (path coefficients: 0.30~0.39) to physiochemical indicators of EC, Turb, and WST in eastern and northern China (i.e., IMXL, NPML, and EPL). The response of pCO_2 to nutrients was strongest in the IMXL zone and weakest in the NPML zone. However, climatic factors had almost no influence on F_c in the YGPL zone, which differed from the other lake zones.

Therefore, results from this study led us to conclude that water quality management initiatives used to improve surface water acidification and hypoxia would simultaneously reduce C emissions while increasing the C sink capacity of China's inland lakes and reservoirs. At a larger regional scale, the CO_2 evasion rate weighed by water surface area exhibited a significant positive correlation with regional mean air temperature (Figure S12, Supplemental Information S7), which indicated that climate warming would promote CO_2 emissions from China's inland lakes and reservoirs. Especially in the IMXL and TPL zones, rising temperatures coupled with increasing precipitation would accelerate the melt of ices and snows and the release of organic C stored in glacier ice, which could speed up the C emissions into the atmosphere.[39,40]

DISCUSSION

Spatiotemporal F_c patterns

Statistically, lakes/reservoirs with higher diurnalCO_2 emissions were more than those with higher nocturnal CO_2 emissions in our dataset. The higher diurnal CO_2 emissions observed from China's lakes and reservoirs were contrasted with those observed from rivers globally.[19,41] The diurnal variation pattern was consistent with directly observed F_c values in certain typical lakes and reservoirs in China.[34,42,43] This may be attributed to higher daytime WS and gas transfer velocity, which could enhance daytime CO_2 emissions from lakes and reservoirs.[16]

Results from this study reveal seasonal F_c patterns at a national scale for the first time. We found that 34% of sampled lakes and reservoirs (i.e., 70 out of 205) transformed from C sources to C sinks within a year. Furthermore, seasonal F_c patterns varied regionally. For example, F_c values in the EPL and TPL zones were higher in summer and autumn and lower in spring and winter, while F_c values in the NPML, IMXL, and YGPL zones were higher in spring and winter and lower in summer and autumn (Figure 3A). Additionally, significant seasonal F_c fluctuations were observed among the five lake zones, where peak values exceeded valley values by factors of 1.5~2.8 across different seasons and regions. Apart from regional and seasonal differentiation, F_c was also found to be dependent on lake area size. Compared with medium-sized lakes and reservoirs (10~50 km[2]), small (<10 km[2]) and large (>50 km[2]) lakes and reservoirs tended to emit higher amounts of CO_2 to the atmosphere (Figure 3B). The higher flux observed from small lakes and reservoirs may be attributed to their high sediment yields and frequent mixing;[25] while for large lakes and reservoirs, higher flux may be caused by high DOC concentrations.[44]

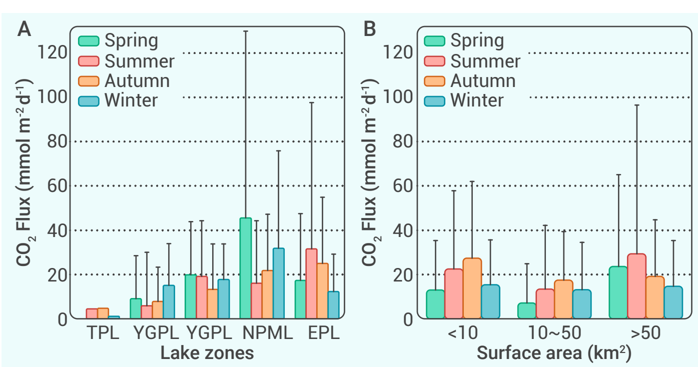

Figure 3. Seasonal distribution of F_c across lake zone (A) and area size categories (B) Error bars denote corresponding standard deviations. Refer to Figure 2 for definitions of lake zones and seasons.

Uncertainties and limitations

Compared with the estimates of 7.9~25 Tg C yr^{-1} from literatures (Table 1),[17,18,21] our state-of-the-art estimate (6.78 Tg C yr^{-1}) was relatively low. Multiple factors are attributed to this estimate discrepancy. Firstly, previous estimates did not account for diurnal and seasonal F_c variations. Currently, all largescale CO_2 emission estimates from China's inland waterbodies are dependent on the limited F_c measurements collected from relevant studies, most of which were sampled during daytime hours, and the seasonal distribution was not homogeneous (fewer observations in winter). As we have demonstrated higher daytime F_c and lower wintertime F_c in China's lakes and reservoirs (Figure 1 and 2), which could partially explain the evidently higher CO_2 flux estimated by previous studies. Secondly, there exists a wide discrepancy in evaluation periods. Considering that F_c measurements collected from the literature may have been sampled during different years, previous estimates can only be used to indicate CO_2 emission levels over extended time periods (i.e., typically at a decadal scale). The latest estimates from the literature are from the 2010s.[18,21] The estimate obtained from our study utilized sampled data from 2021 to 2022, which thus provides an up-to-date assessment of CO_2 emissions from China's inland lakes and

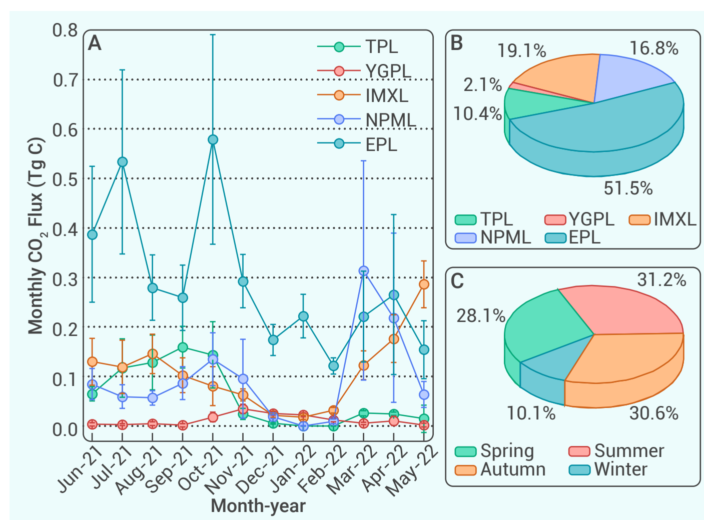

Figure 4. Spatiotemporal variations in total CO_2 emissions across all five lake zones (A) Monthly variation of regional CO_2 emissions; (B) proportional distribution of annual CO_2 flux across five lake zones; (C) proportional distribution of seasonal CO_2 flux. Refer to Figure 2 for definitions of lake zones and seasons.

Table 1. Comparison among documented CO_2 emission estimates from China's lakes and reservoirs.

Water surface area (×10[5] km[2])	Annual CO_2 flux (Tg C yr^{-1})	Sampling period	Reference
0.94~1.05	**6.78 (±2.5)**	**2021–2022**	**This study**
1.2	7.9 (±10.4)	2010s	Wang et al., 2023 [17]
1.08	12.1 (±2.1)	2010s	Ran et al., 2021 [14]
1.09	25.15 (±4.3)	2000–2014	Li et al., 2018 [13]
0.94	9.4 (±1.8)	1980s	Ran et al., 2021 [14]

Note: numbers in parentheses represent standard deviations or confidence intervals.

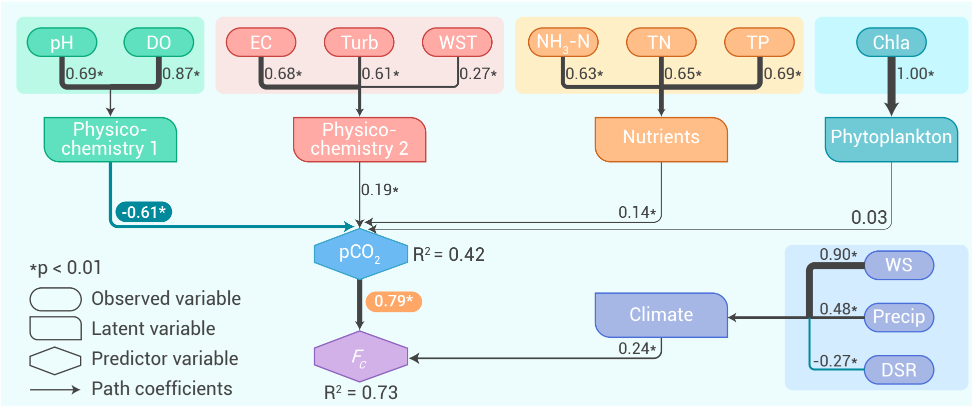

Figure 5. Environmental controls on pCO_2 and F_c from China's lakes and reservoirs The full environmental indicator names are as follows: pondus hydrogenii (pH), dissolved oxygen (DO), electrical conductivity (EC), turbidity (Turb), water surface temperature (WST), ammonia nitrogen (NH_3-N), total nitrogen (TN), total phosphorus (TP), chlorophyll *a* (Chl-*a*), wind speed (WS) at a 10 m height, total precipitation (Precip), and downward solar radiation (DSR).

reservoirs. Thirdly, previous estimates have rarely considered seasonal surface area fluctuations from lakes and reservoirs. In reality, impacts of water surface area variation on areal CO_2 emission assessments may be consequentially exceptional in some flood-prone lakes and regulated reservoirs.[23] China's largest freshwater lake (Poyang Lake) is an example, where total CO_2 flux can reach up to 0.43 Tg C yr^{-1}. However, the dynamic range of Poyang Lake's monthly inundation area varies widely (1116~2578 km^2). Therefore, estimated CO_2 flux from Poyang Lake would range from 0.22 Tg C yr^{-1} to 0.52 Tg C yr^{-1} without accounting for monthly inundation area dynamics (Figure S9, Supplemental Information S6).

Upscaling CO_2 flux from site to regional scales will result in considerable and unavoidable uncertainty. This mainly transpires from errors in the estimation of pCO_2, gas transfer velocity (k), and water surface area. Accordingly, we performed a Monte Carlo analysis to quantify variance in our estimate on regional CO_2 flux by providing uncertainty intervals for these three statistically independent components of error sources, and then randomly picked up values from the intervals for 10,000 iterations to obtain the distribution of the simulated estimates (Table S5, Supplemental Information S6). Overall, the simulation predicted a mean flux of 6.71 Tg C yr^{-1} and a median flux of 5.82 Tg C yr^{-1}, under a large uncertainty range (1.2~14.8 Tg C yr^{-1}, 5^{th} and 95^{th} confidence interval percentiles). The mean flux of our simulated results was very close to the estimated flux of 6.78 Tg C yr^{-1}. Regionally, differences between estimated flux and simulated mean flux ranged between -0.21 Tg C yr^{-1} and 0.11 Tg C yr^{-1} across all five lake zones, which was relatively small (<20%) compared to regional CO_2 flux. The consistency between estimated and simulated flux at both regional and national scales demonstrated the high confidence of this proposed approach for CO_2 flux estimations in China's inland lakes and reservoirs.

The TPL zone covers nearly half of China's lake surface area. However, because this zone has only one sampling site, significant CO_2 emission evaluation bias may result. TPL presented as a C source in our estimate, with a flux of 0.71 Tg C yr^{-1}. This is comparable to a recent estimate of 1.16 Tg C yr^{-1} by Jia et al. (2022), which was calculated using samples collected from 41 lakes and three reservoirs in 2020.[45] This estimate is obviously lower than the estimate of 3.87 Tg C yr^{-1} by Ran et al. (2021), which was calculated by literature derived data in the 2010s.[18] It was also noted that saline lakes in the TPL were estimated to be a large C sink with a flux of -10.28±1.65 Tg C yr^{-1} by eddy covariance method;[46] while water chemistry records and headspace equilibration method derived estimates suggested that TPL lakes was a large C source.[47] Given the significant geographical, climatological, physical, and chemical diversity of lakes and reservoirs in the TPL zone, quantifying its total CO_2 flux remains challenging, requiring more observations with long period, high frequency and different methods.

Implications for China's terrestrial C budget

Being important reactors and regulators of C emissions, C storage, and C transportation, the total C emitted, accumulated, and transported from lakes and reservoirs may have a consequential effect on the terrestrial C balance.[5] This study estimated C flux from China's lakes and reservoirs at 6.78 Tg C yr^{-1} during the 2020s, accounting for both spatiotemporal variation in the F_c and water surface area. This estimate accounted for 7~11% of CO_2 emissions from China's inland waterbodies during the 2010s[18,21] and approximately 2% of CO_2 emissions from global lakes and reservoirs (Table 1).[13] It should be noted that phytoplankton widely distributed in lakes and reservoirs could absorb a large amount of CO_2 via photosynthesis.[48,49] The total C sequestration capacity by phytoplankton (indicated by gross primary productivity [GPP]) respective to China's inland lakes and reservoirs was estimated at 19.41 Tg C yr^{-1}.[50] If transported and buried C are ignored in the estimates (allowing for the fact that no accurate estimations currently exist), China's inland lakes and reservoirs over recent years could be regarded as a large C sink, with a C sequestration capacity of 12.63 Tg C yr^{-1}. Owing to the absence of accurate C emission estimates, the C cycle processes of inland waters, including rivers, lakes and reservoirs, have largely been ignored in the C budget estimations of China's terrestrial ecosystems. China's terrestrial C sink (regardless of inland waters) during the past two decades was 170~350 Tg C yr^{-1},[51] which could increase by 3.6~7.4% when accounting for the C sink of lakes and reservoirs.

CONCLUSIONS

This study proposed a novel approach to track spatial and temporal dynamics of CO_2 flux from China's lakes and reservoirs using nationwide real-time water quality monitoring data and machine learning models. Accounting for the spatiotemporal variability in F_c and water surface area, this study estimated the total CO_2 emission rate at 6.78 Tg C yr^{-1} (2021–2022), which is obviously lower than previous estimates, ranging from 7.9 to 25 Tg C yr^{-1} (1980s–2010s). Nevertheless, neglecting lake and reservoir CO_2 flux could result in non-negligible bias in the C budget of China's terrestrial ecosystems. This study also provided new scientific insight into environmental controls on CO_2 emissions from China's lakes and reservoirs. pH and DO were identified as the general controls of water-air interface CO_2 exchange. Climate warming could also accelerate reginal CO_2 emission rates. Thus, results from this study demonstrated that water quality control and climate warming mitigation will synergistically reduce C emissions while increasing the C sink capacity of China's inland lakes and reservoirs.

MATERIALS AND METHODS

Site level CO_2 flux (F_c, mmol m^{-2} d^{-1}) across the water-air interface was determined using the following equation:

$$F_c = k \times k_H \times \Delta pCO_2 \quad (1)$$

where k is the gas transfer velocity (cm h^{-1});k_H is the Henry's law constant adjusted for water temperature (mol L^{-1} atm^{-1}); ΔpCO_2 represents the difference in pCO_2 between water and the atmosphere (μatm). A positive ΔpCO_2 value indicates that waterbodies emit CO_2 to the atmosphere whereas a negative value indicates that waterbodies absorb CO_2 from the atmosphere. k was determined from optimal empirical models based on WS (Supplemental Information S5).[18] These empirical models have been validated under different climatic and hydrologic conditions throughout China. Modeled k values generally agreed well with direct k measurements using floating chambers in the lakes and reservoirs of the EPL and TPL zones (R^2=0.64, p<0.001).[18] Atmospheric pCO_2 was obtained from NOAA's Global Greenhouse Gas Reference Network of the Earth System Research Laboratory (ESRL). pCO_2 content in water was determined from water chemistry records (i.e., pH, WST, and alkalinity [Alk]) using CO2SYSv3 software.[52] pH and WST, sampled and measured at a 4-h frequency, were obtained from the China National Environmental Monitoring Centre (CNEMC) between June 2021 and May 2022.

Alk was estimated using five indicators (pH, DO, EC, TN, and TP) from CNEMC with a machine learning model, namely, Random Forest with bagged trees (RF-BAT), which was trained using the GLObal RIver CHemistry database (GLORICH) and validated using in situ measurements from typical lakes in China (Figure S3–4, Table S2–3). pCO_2 overestimations in water under low pH (<6.5) and Alk (<1000 μeq/L) conditions were corrected using an empirical model developed by Liu et al. (2020).[53] The pCO_2 estimated from water chemistry data showed good agreement with direct measurements by headspace equilibration method (Figure S6).

Accounting for the fact that pCO_2 and k are highly dependent on region, time, and surface area size,[14,18,54,55] China's inland lakes and reservoirs were divided into five lake zones (i.e., TPL, YGPL, IMXL, NPML, and EPL) according to their specific geographic, topographic, and climatic diversity (Figure S1).[56] Lakes and reservoirs were simultaneously divided into three different size categories according to surface area differences (i.e., <10, 10–50, and >50 km^2).[18] We calculated areal CO_2 flux (F_c^T, in Tg C) by surface area size and day within each lake zone using the following formula:

$$F_c^T = \sum_{Region}\left[\sum_{class}\left(\sum_{day}\left(\bar{F_c} \times SA\right)\right)\right] \quad (2)$$

where $\bar{F_c}$ is the daily and regional mean F_c of a specific lake/reservoir area size within a lake zone. *SA* is the monthly surface area of lakes and reservoirs, which was obtained from the satellite-based Reservoir and Lake Surface Area Timeseries (ReaLSAT) dataset.[57] Allowing for the fact that ice cover may prevent atmospheric exchange and subsequently lead to CO_2 accumulation, frozen lakes/reservoirs were excluded from our F_c^T calculation. Ice-covered areas were identified based on daily mean air temperature (AT), under the assumption that lakes/reservoirs were fully covered by ice when AT was less than -4°C.[13] The influence of ice cover on CO_2 emissions was quantified by comparing flux differences with and without ice cover (Table S4). A Monte Carlo simulation was used to evaluate the uncertainty associated with F_c^T calculations (Table S5).

See Supplemental Information for more detail on the materials and methods used in this study.

REFERENCES

1. Cole, J.J., Prairie, Y.T., Caraco, N.F., et al. (2007). Plumbing the Global Carbon Cycle: Integrating Inland Waters into the Terrestrial Carbon Budget. Ecosystems *10*, 172–185.
2. Battin, T.J., Luyssaert, S., Kaplan, L.A., et al. (2009). The boundless carbon cycle. Nat. Geosci. *2*, 598–600.
3. Regnier, P., Resplandy, L., Najjar, R.G., and Ciais, P. (2022). The land-to-ocean loops of the global carbon cycle. Nature *603*, 401–410.
4. Koehler, B., Landelius, T., Weyhenmeyer, G.A., et al. (2014). Sunlight-induced carbon dioxide emissions from inland waters. Glob. Biogeochem. Cycle. *28*, 696–711.
5. Pilla, R.M., Griffiths, N.A., Gu, L., et al. (2022). Anthropogenically driven climate and landscape change effects on inland water carbon dynamics: What have we learned and where are we going. Glob. Change Biol. *28*, 5601–5629.
6. Borges, A.V., Darchambeau, F., Lambert, T., et al. (2018). Effects of agricultural land use on fluvial carbon dioxide, methane and nitrous oxide concentrations in a large European river, the Meuse (Belgium). Sci. Total Environ. *610-611*, 342-355.
7. Borges, A.V., Darchambeau, F., Lambert, T., et al. (2019). Variations in dissolved greenhouse gases (CO2, CH4, N2O) in the Congo River network overwhelmingly driven by fluvial-wetland connectivity. Biogeosciences *16*, 3801–3834.
8. Borges, A.V., Okello, W., Bouillon, S., et al. (2023). Spatial and temporal variations of dissolved CO2, CH4 and N2O in Lakes Edward and George (East Africa). J. Gt. Lakes Res. *49*, 229–245.
9. Xiao, W., Liu, S., Li, H., et al. (2014). A Flux-Gradient System for Simultaneous Measurement of the CH4, CO2, and H2O Fluxes at a Lake–Air Interface. Environ. Sci. Technol. *48*, 14490–14498.
10. Shi, W., Chen, Q., Yi, Q., et al. (2017). Carbon Emission from Cascade Reservoirs: Spatial Heterogeneity and Mechanisms. Environ. Sci. Technol. *51*, 12175–12181.
11. Xu, Y.J., Xu, Z., and Yang, R. (2019). Rapid daily change in surface water pCO2 and CO2 evasion: A case study in a subtropical eutrophic lake in Southern USA. J. Hydrol. *570*, 486–494.
12. Yang, R., Xu, Z., Liu, S., and Xu, Y.J. (2019). Daily pCO2 and CO2 flux variations in a subtropical mesotrophic shallow lake. Water Res. *153*, 29–38.
13. Raymond, P.A., Hartmann, J., Lauerwald, R., et al. (2013). Global carbon dioxide emissions from inland waters. Nature *503*, 355–359.
14. Golub, M., Koupaei-Abyazani, N., Vesala, T., et al. (2023). Diel, seasonal, and inter-annual variation in carbon dioxide effluxes from lakes and reservoirs. Environ. Res. Lett. *18*, 034046.
15. Campbell, A.D., Fatoyinbo, T., Charles, S.P., et al. (2022). A review of carbon monitoring in wet carbon systems using remote sensing. Environ. Res. Lett. *17*, 025009.
16. Borges, A.V., Deirmendjian, L., Bouillon, S., et al. (2022). Greenhouse gas emissions from African lakes are no longer a blind spot. Sci. Adv. *8*, eabi8716.
17. Li, S., Bush, R.T., Santos, I.R., et al. (2018). Large greenhouse gases emissions from China's lakes and reservoirs. Water Res. *147*, 13–24.
18. Ran, L., Butman, D.E., Battin, T.J., et al. (2021). Substantial decrease in CO2 emissions from Chinese inland waters due to global change. Nat. Commun. *12*, 1730.
19. Gómez-Gener, L., Rocher-Ros, G., Battin, T., et al. (2021). Global carbon dioxide efflux from rivers enhanced by high nocturnal emissions. Nat. Geosci. *14*, 289–294.
20. Liu, S., Kuhn, C., Amatulli, G., et al. (2022). The importance of hydrology in routing terrestrial carbon to the atmosphere via global streams and rivers. Proc. Natl. Acad. Sci. U. S. A. *119*, e2106322119.
21. Wang, J., Zhou, Y., Zhou, L., et al. (2023). Urbanization in developing countries overrides catchment productivity in fueling inland water CO2 emissions. Glob. Change Biol. *29*, 1–4.
22. Donchyts, G., Winsemius, H., Baart, F., et al. (2022). High-resolution surface water dynamics in Earth's small and medium-sized reservoirs. Sci Rep. *12*, 13776.
23. Pi, X., Luo, Q., Feng, L., et al. (2022). Mapping global lake dynamics reveals the emerging roles of small lakes. Nat. Commun. *13*, 5777.
24. Keller, P.S., Marcé, R., Obrador, B., and Koschorreck, M. (2021). Global carbon budget of reservoirs is overturned by the quantification of drawdown areas. Nat. Geosci. *14*, 402–408.
25. Holgerson, M.A., and Raymond, P.A. (2016). Large contribution to inland water CO2 and CH4 emissions from very small ponds. Nat. Geosci. *9*, 222–226.
26. Aufdenkampe, A.K., Mayorga, E., Raymond, P.A., et al. (2011). Riverine coupling of biogeochemical cycles between land, oceans, and atmosphere. Front. Ecol. Environ. *9*, 53–60.
27. Pu, J., Li, J., Zhang, T., et al. (2020). Varying thermal structure controls the dynamics of CO2 emissions from a subtropical reservoir, south China. Water Res. *178*, 115831.
28. Xiao, Q., Xu, X., Duan, H., et al. (2020). Eutrophic Lake Taihu as a significant CO2 source during 2000–2015. Water Res. *170*, 115331.
29. Guo, Y., Zhang, Y., Ma, N., et al. (2022). Significant CO2 sink over the Tibet's largest lake: Implication for carbon neutrality across the Tibetan Plateau. Sci. Total Environ. *843*, 156792.
30. Wang, S., Gao, Y., Jia, J., et al. (2022). Determining whether hydrological processes drive carbon source and sink conversion shifts in a large floodplain-lake system in China. Water Res. *224*, 119105.
31. Song, K., Wen, Z., Shang, Y., et al. (2018). Quantification of dissolved organic carbon (DOC) storage in lakes and reservoirs of mainland China. J. Environ. Manage. *217*, 391–402.
32. Zhou, N., Liu, Z., Liu, K., et al. (2022). Carbon, nitrogen, and phosphorus dynamics in China's lakes: climatic and geographic influences. Environ. Monit. Assess. *195*, 113.
33. Qu, L., He, C., Wu, Z., et al. (2022). Hypolimnetic deoxygenation enhanced production and export of recalcitrant dissolved organic matter in a large stratified reservoir. Water Res. *219*, 118537.
34. Yang, P., Wang, N.a., Zhao, L., et al. (2021). Variation characteristics and influencing mechanism of CO2 flux from lakes in the Badain Jaran Desert: A case study of Yindeer Lake. Ecol. Indic. *127*, 107731.
35. Xiao, Q., Duan, H., Qin, B., et al. (2022). Eutrophication and temperature drive large variability in carbon dioxide from China's Lake Taihu. Limnol. Oceanogr. *67*, 379–391.
36. Lu, Y., Gao, Y., Jia, J., et al. (2022). Water Conveyance-Type Lake Systems Shift toward Carbon Sources under Regulatory Balanced Water Level Metabolic Processes. ACS Earth Space Chem. *6*, 2400–2411.
37. Zhang, J., Jiang, Y., Gao, Y., et al. (2013). CO2 emission from Dianshan Lake in summer, East China. Chin. J. Geochem. *32*, 430–435.
38. Wen, Z., Song, K., Shang, Y., et al. (2017). Carbon dioxide emissions from lakes and reservoirs of China: A regional estimate based on the calculated pCO2. Atmos. Environ. *170*, 71–81.
39. Hood, E., Battin, T.J., Fellman, J., et al. (2015). Storage and release of organic carbon from glaciers and ice sheets. Nat. Geosci. *8*, 91–96.
40. Wang, J., Hilton, R.G., Jin, Z., et al. (2019). The isotopic composition and fluxes of particulate organic carbon exported from the eastern margin of the Tibetan Plateau. Geochim. Cosmochim. Acta *252*, 1–15.
41. Attermeyer, K., Casas-Ruiz, J.P., Fuss, T., et al. (2021). Carbon dioxide fluxes increase from day to night across European streams. Commun. Earth Environ. *2*, 118.
42. Xiao, S., Wang, Y., Liu, D., et al. (2013). Diel and seasonal variation of methane and carbon dioxide fluxes at Site Guojiaba, the Three Gorges Reservoir. J. Environ. Sci. *25*, 2065–2071.
43. Zhang, Z., Yu, R., Xia, X., et al. (2022). Significant diurnal variation of CO2 flux from a shallow eutrophic lake: effects of submerged aquatic vegetation and algae bloom. Aquat. Sci. *84*, 62.
44. Humborg, C., MÖRth, C.-M., Sundbom, M., et al. (2010). CO2 supersaturation along the aquatic conduit in Swedish watersheds as constrained by terrestrial respiration, aquatic respiration and weathering. Glob. Change Biol. *16*, 1966–1978.
45. Jia, J., Sun, K., Lü, S., et al. (2022). Determining whether Qinghai–Tibet Plateau waterbodies have acted like carbon sinks or sources over the past 20 years. Sci. Bull.

67, 2345–2357.
46. Li, X.-Y., Shi, F.-Z., Ma, Y.-J., et al. (2022). Significant winter CO2 uptake by saline lakes on the Qinghai-Tibet Plateau. Glob. Change Biol. *28*, 2041–2052.
47. Yan, F., Sillanpää, M., Kang, S., et al. (2018). Lakes on the Tibetan Plateau as Conduits of Greenhouse Gases to the Atmosphere. J. Geophys. Res.-Biogeosci. *123*, 2091–2103.
48. Staehr, P.A., Testa, J.M., Kemp, W.M., et al. (2012). The metabolism of aquatic ecosystems: history, applications, and future challenges. Aquat. Sci. *74*, 15–29.
49. Jia, J., Gao, Y., Qin, B., et al. (2022). Evolving geographical gross primary productivity patterns in global lake systems and controlling mechanisms of associated phytoplankton communities since the 1950s. Earth-Sci. Rev. *234*, 104221.
50. Gao, Y., Jia, J., Lu, Y., et al. (2021). Determining dominating control mechanisms of inland water carbon cycling processes and associated gross primary productivity on regional and global scales. Earth-Sci. Rev. *213*, 103497.
51. Piao, S., He, Y., Wang, X., and Chen, F. (2022). Estimation of China's terrestrial ecosystem carbon sink: Methods, progress and prospects. Sci. China-Earth Sci. *65*, 641–651.
52. Sharp, J.D., Pierrot, D., Humphreys, M.P., et al. (2021). CO2SYSv3 for MATLAB (v3.2.0). Zenodo. https://doi.org/10.5281/zenodo.4774718.
53. Liu, S., Butman, D.E., and Raymond, P.A. (2020). Evaluating CO2 calculation error from organic alkalinity and pH measurement error in low ionic strength freshwaters. Limnol. Oceanogr. Meth. *18*, 606–622.
54. Read, J.S., Hamilton, D.P., Desai, A.R., et al. (2012). Lake-size dependency of wind shear and convection as controls on gas exchange. Geophys. Res. Lett. *39*, L09405.
55. Kankaala, P., Huotari, J., Tulonen, T., and Ojala, A. (2013). Lake-size dependent physical forcing drives carbon dioxide and methane effluxes from lakes in a boreal landscape. Limnol. Oceanogr. *58*, 1915–1930.
56. Ma, R., Duan, H., Hu, C., et al. (2010). A half-century of changes in China's lakes: Global warming or human influence. Geophys. Res. Lett. *37*, L045514.
57. Khandelwal, A., Karpatne, A., Ravirathinam, P., et al. (2022). ReaLSAT, a global dataset of reservoir and lake surface area variations. Sci. Data *9*, 356.

ACKNOWLEDGMENTS

The authors would like to thank CNEMC for providing the water quality monitoring data used in this study. This study was financially supported by the CAS Project for Young Scientists in Basic Research (Grant No. YSBR-037) and National Nature Science Foundation of China (No. 42225103, 42141015 and 31988102) and the Open Research Fund of the State Key Laboratory of Simulation and Regulation of Water Cycle in River Basin, the China Institute of Water Resources and Hydropower Research (Grant No. IWHR-SKL-202210).

AUTHOR CONTRIBUTIONS

K.S. and Y.G. initiated this study and led the writing of the manuscript. K.S., J.J. and S.W. performed the data processing and analysis. All authors participated in the discussion and writing.

DECLARATION OF INTERESTS

The authors declare no competing interests.

SUPPLEMENTAL INFORMATION

It can be found online at https://doi.org/10.59717/j.xinn-geo.2023.100031

LEAD CONTACT WEBSITE

http://www.igsnrr.cas.cn/sourcedb_igsnrr_cas/zw/zjrck/qcqn/201404/t20140409_4087651.html